Chemical composition of particulate matter from traffic emissions in a road tunnel in Xi'an, China

Yanzhao Hao[1], Shunxi Deng[2, 4*], Yan Yang[3, 4], Wenbin Song[5], Hui Tong[4], Zhaowen Qiu[1]

[1] *School of Automobile, Chang'an University, Xi'an 710064, China*
[2] *Key Laboratory of Subsurface Hydrology and Ecological Effect in Arid Region of Ministry of Education, Chang'an University, Xi'an 710064, China*
[3] *Chinese Research Academy of Environmental Sciences, Beijing 100012, China*
[4] *School of Environmental Science and Engineering, Chang'an University, Xi'an 710064, China*
[5] *Xi'an Environmental Protection Bureau, Xi'an 710054, China*

ABSTRACT

Chemical composition of particulate matter (PM) from traffic emissions vary by region and time. Therefore, it is necessary to obtain local mobile source profiles of PM to support regional researches for vehicle emission control policy, source apportionment modeling, etc. In this study, $PM_{2.5}$ and PM_{10} samples were collected from a highway tunnel in Xi′an, northwestern China. Detailed chemical composition, including OC, EC, water-soluble ions, and elements, were analyzed to (1) provide a local PM profile with mixed vehicle fleet, (2) identify the origins of different elements in the tunnel environment, and (3) determine the associated factors influencing PM profiles. The $PM_{2.5}$ profiles in the tunnel included OC (34.10%), EC (11.96%), water-soluble ions (18.22%), and elements (27.73%), while the PM_{10} profiles included OC (28.48%), EC (8.59%), water-soluble ions (14.17%), and elements (33.36%). The origins of the elements in the tunnel were classified into three categories by the receptor modeling approach, which included resuspended road dust and brake wear, vehicle exhaust and tire wear, and tailpipe emissions from diesel vehicles (DV).The mass fractions of OC, EC, and elements originating from resuspended road dust and brake wear were mainly affected by vehicle driving conditions (i.e., uphill/downhill and speed), whereas the mass content of bromine (Br) was influenced by the proportion of DV in the fleet.

Keywords: Traffic emissions; $PM_{2.5}$; PM_{10}; Source profile; Road tunnel

[*]Corresponding author. Tel./fax: + 86 29 82334207
E-mail address: dengshunxi@aliyun.com

INTRODUCTION

Particulate matter (PM) is a primary pollutant of atmospheric haze pollution in China, which has an adverse impact on public health, especially on human lungs and hearts (Delfino et al., 2008; Liu et al., 2015a; Spira-Cohen et al., 2011). Motor vehicles are a major source of PM in the atmosphere. According to the official source apportionment results of $PM_{2.5}$ in 15 cities of China (MEPC, 2017), the contribution of motor vehicles in 11 cities was greater than 20%, with an average value of 23.36%. In order to better control PM pollution, it is essential to understand the physical and chemical characteristics of the PM emitted from motor vehicles. Vehicle emissions can be investigated using various testing methods, such as the tunnel test (Alves et al., 2015a; Pio et al., 2013), dynamometer test (Na et al., 2015; Pietikainen et al., 2015), and on-road test (Yao et al., 2015; Zhang et al., 2015a). Compared with other approaches, tunnel test can easily obtain the emission characteristics of PM with mixed vehicle fleet under actual driving conditions (Franco et al., 2013; Pant et al., 2017). Further, PM pollutants collected in the tunnel include not only vehicle exhaust, but also some associated emissions, such as friction emissions (tire, brake, and road surface wear) and road dust (Handler et al., 2008; Thorpe and Harrison, 2008). Therefore, tunnel test can estimate the PM pollution caused by motor vehicles more comprehensively.

Faced with the increasingly serious air pollution problem, several studies have been conducted on the chemical characteristics of PM from vehicle emissions by means of tunnel tests in China. Most of these studies were carried out in the eastern part of China, mainly in Guangzhou (Dai et al., 2015; Huang et al., 2006; He et al., 2008; Zhang et al., 2015b), Hong Kong (Chiang and

Huang, 2009; Cheng et al., 2010; Ho et al., 2009), and Shanghai (Zhao et al., 2010; Liu et al., 2015b; Liu et al., 2015c).However, no such studies have been conducted in the western part of China, such as Xi′an, which is the capital of Shaanxi province (Fig. 1). Xi′an is the largest city in northwestern China, with up to 2.42 million licensed vehicles in 2015. Moreover, vehicle emission was the second largest source of $PM_{2.5}$ pollution in Xi′an, with contributions of 14.9% and 12.9% in urban and rural areas, respectively (Wang et al., 2015).Considering that each region has its own characteristic vehicular fleet (vehicle type, fuel quality, etc.) and corresponding conditions (transportation infrastructure, driving conditions, etc.) that influence vehicular emissions, it is important to conduct local studies to obtain local emission profiles (Alves et al., 2016; Zhang et al., 2015b).

This study carried out a tunnel experiment in Xi′an, with the following objectives: (1) investigate the chemical characteristics of PM in a typical highway tunnel, and obtain the local mobile source profiles of PM; (2) identify the main sources of each element in PM, such as vehicle exhaust, tire wear, brake wear, and resuspended road dust; and (3) determine the main factors affecting the chemical composition of PM from road traffic. Results from this study will provide necessary data for subsequent studies in northwestern China, such as vehicle emission control policy, source apportionment modeling, and air quality simulation.

MATERIALS AND METHODOLOGY

Sampling sites

The sampling experiment was conducted in the Qinling No. 1 tunnel, which is located in the

84 southwest suburb of Xi'an. There are no significant anthropogenic pollution sources around it,
85 apart from motor vehicles. This highway tunnel has two independent bores (southbound and
86 northbound), each of which has two lanes, as shown in Fig. 1. The southbound bore is 6102 m in
87 length, with an upgrade of +2.58% (Uphill); whereas the northbound bore is 6144 m, with a
88 downgrade of -2.58% (Downhill). A ventilation shaft was placed at 1657 m from the entrance of
89 the northbound bore, which was ventilated naturally during the test. There were four sampling
90 sites in the southbound bore, with three sampling sites in the northbound bore (Fig. 1). More
91 details of the sampling sites are summarized in Section A1 in the supplementary material. The
92 samplers were placed in the emergency parking areas at a distance of 3 m from the nearside lane.
93 This experiment was performed for several purposes, such as determining gas pollution (e.g. CO,
94 NO_x, SO_2, and O_3) and visibility in the tunnel, while this study only focused on the chemical
95 composition of the PM.
96
97 ***Sampling method***
98 The four-channel PM sampler (TH-16A, Tianhong Corporation, Wuhan, China) was used to
99 sample inhalable particles (PM_{10}) and fine particles ($PM_{2.5}$) simultaneously. Two channels were
100 loaded with 47-mm quartz-fiber filters, while the other two were loaded with 47-mm Teflon
101 filters. The operating flow rate was 16.7 L min^{-1}, with a sampling height of 2 m. During this
102 experiment, two samplers were used to collect PM concurrently, one of which was placed at site
103 #1, while the other one was moved day by day from site #2 to site #3, and then to site #4. The
104 duration of each sampling was 6–10 h to ensure that sufficient material was collected, with at
105 least two sets of PM samples being collected at each site. The entire experiment lasted for one

week (March 14–20, 2016), with 20 sampling sets being collected during two daily periods, one was at daytime between 8:00 to 20:00, and the other one was at nighttime between 20:00 to 8:00 (Table 1).

The meteorological parameters at each sampling site were recorded in parallel using an automatic weather station (GH-BPR, Huayun Puda Corporation, Beijing, China). A roadside laser traffic survey instrument (AxleLight RLU11, NanoSense Corporation, Beijing, China) was used to investigate the traffic parameters during the entire test, including vehicle volume, speed and vehicle types.

Mass and chemical analysis

The PM mass concentrations were determined gravimetrically by weighing the filters before and after sampling (an MC5 Sartorius microbalance was used for weighing). Subsequently, the quartz-fiber filter was cut into two pieces to detect the carbonaceous species and water-soluble ions separately, whereas a Teflon filter was used to analyze the elements.

The contents of organic carbon (OC) and elemental carbon (EC) were determined by a model-4L semi-continuous aerosol carbon analyzer (Sunset Laboratory Inc.) with the thermal-optical transmission method (TOT; NIOSH, 2003). The water-soluble ions were analyzed by an ICS-5000 ion chromatograph (Thermo Fisher Inc.), following the method of Zhang et al. (2014). Trace elements were analyzed by an Epsilon-5 X-ray fluorescence spectrometer (PANalytical Inc.). Finally, three ionic species (NH_4^+, NO_3^-, and SO_4^{2-}) and seventeen elements (Na, Mg, Al, P, S, K, Ca, Ti, Cr, Mn, Fe, Cu, Zn, Br, Ba, Hg, and Pb) were identified. More details of the analysis procedure are available in Section A2 in the supplementary material. The

quality assurance and control of chemical analysis are summarized in Section A3 in the supplementary material.

Statistical analysis

Data analysis was performed using SPSS (Version 17). Species' correlation analysis was conducted based on Pearson Correlation. Multivariate analysis of variance (Multivariate-ANOVA) was carried out to test for significant variations in chemical composition between $PM_{2.5}$ and PM_{10} (Haase and Ellis, 1987). Moreover, the receptor modeling approach, including enrichment factor (EF) and principal component analysis (PCA), were adopted to identify the main sources of elements in the PM. Enrichment factor (EF) is a good indicator of the contributions of anthropogenic sources (Cevik, et al., 2009). It is calculated by the following equation:

$$EF_i = \frac{(C_i/C_r)_{Tunnel}}{(C_i/C_r)_{Background}} \quad (1)$$

where EF_i is the enrichment factor of element *i,* C_i is the concentration of element *i*, C_r is the concentration of the reference element, tunnel and background represent the sampling sources of the elements. Aluminum (Al) was selected as the reference element in this study (Sakan et al., 2014), while the average background concentrations of elements in the soil of A layer in Shaanxi province were considered as the background values in this calculation (NEMCC, 1990).

PCA is a factor analysis method, which is a useful tool to apportion the emission sources and quantify their contributions (Larsen and Baker, 2003). In PCA, all factors with eigenvalues over 1 were extracted and rotated using the Varimax method. Each of these factors can be identified as either an emission source or a chemical interaction. In order to determine the suitability of the

dataset for PCA, a Kaiser-Meyer-Olkin (KMO) value of greater than 0.6 was required (Lawrence et al., 2013). High values (close to 1) usually indicate that the PCA is useful with the selected dataset. Finally, the multifactorial analysis of variance (Multifactorial-ANOVA) was applied to analyze the main influential factors on PM composition in the tunnel (Wolny and Kedzia, 2008).

RESULTS AND DISCUSSION

Chemical composition of PM

The chemical compositions of $PM_{2.5}$ and PM_{10} were analyzed separately in this study. The results are summarized in Table 2. Moreover, the results of Multivariate-ANOVA showed that the chemical compositions between $PM_{2.5}$ and PM_{10} were statistically distinct (the p-values from all the four tests, i.e. Pillai's Trace, Wilks' Lambda, Hotelling's Trace, and Roy's Largest Root, were 0.001 less than 0.05). Moreover, EC and the elements of Na, Mg, Ca, Ti, Cu, Zn, and Ba were significantly influenced by particle size (Table 3). The mass fraction of EC in $PM_{2.5}$ was higher than that in PM_{10}, whereas the fractions of Na, Mg, Ca, Ti, Cu, Zn, and Ba in $PM_{2.5}$were lower than those in PM_{10}.

OC and EC

The mass fractions of OC and EC in $PM_{2.5}$ were 34.10±6.43%(mean±sd, n=20) and 11.96±4.30%, while their counterparts in PM_{10} were 28.48±16.02% and 8.59±3.81%.The mass ratios of OC/EC in $PM_{2.5}$ and PM_{10} were 2.99±1.11 and 3.30±1.28, respectively, which showed that the contents of OC were noticeably higher than those of EC. EC is formed due to the incomplete combustion of fuel, and it can be emitted from motor vehicles directly. However,

sources of OC are relatively complex, including the primary organic carbon (POC) directly emitted by motor vehicles and secondary organic carbon (SOC) produced from the gaseous precursors (Shen et al., 2011). SOC generation is usually considered to occurwhen the mass ratio of OC/EC is greater than 2 (Deng et al., 2013; Yu et al., 2004). On the other hand, significant correlations were observed between OC and EC ($r_{PM_{2.5}}$=0.91, $r_{PM_{10}}$=0.90), suggesting a similar origin (i.e., direct emissions from motor vehicles) for both.

Water-soluble ions

The mass fractions of NH_4^+, NO_3^-, and SO_4^{2-}in $PM_{2.5}$were 3.19±2.04% (n=20), 6.05±4.42%, and 8.98±4.82%, while those in PM_{10} were 2.14±1.54%, 4.30±2.97%, and 7.73±4.40%. The order of the three ions in terms of their contents from highest to lowest was SO_4^{2-}> NO_3^-> NH_4^+. Usually, NH_4^+, NO_3^-, and SO_4^{2-}can be called secondary ions, which are mainly derived from the gas-to-particle conversion of gaseous precursors (NH_3, NO_x, and SO_2), subsequently being coagulated in the PM in the form of $(NH_4)_2SO_4$, NH_4HSO_4, and NH_4NO_3 (Seinfeld and Pandis, 2016). In this study, NH_4^+ was more strongly correlated with SO_4^{2-} ($r_{PM_{2.5}}$=0.95, $r_{PM_{10}}$=0.91) than NO_3^-($r_{PM_{2.5}}$=0.72, $r_{PM_{10}}$=0.70). It's likely because that the NH_4NO_3 is more easily volatile into gas phase again due to its strong volatility (Chow, 1995). Moreover, it also indicated that the NH_4^+in the PM sampled in this tunnel was primarily in the form of $(NH_4)_2SO_4$ or NH_4HSO_4.

Elements

The elements can be classified into five groups (>5%, 1–5%, 0.1–1%, 0.01–0.1%, and <0.01%), in terms of their mass fractions (Table 4). It can be seen that the mass fraction of each element

196 varied significantly. S was the most abundant element (16.00±7.64% for $PM_{2.5}$ and 12.89±4.77%
197 for PM_{10}, n=20), followed by Al, Mg, Fe, Ca, and Na. These six elements accounted for 95.68%
198 and 95.15% of the total mass of the 17 elements in $PM_{2.5}$ and PM_{10}, respectively.
199
200 Elements can be categorized into metallic and non-metallic (Fig. 2). The non-metallic elements
201 accounted for 58.59% and 39.42% of the total mass of the 17 elements in $PM_{2.5}$ and PM_{10},
202 respectively, with S being the most abundant element. Meanwhile, the mass fractions of metallic
203 elements were 41.41% and 60.58%, with Al, Mg, and Fe being the most abundant elements.
204 Moreover, metallic elements can be further categorized into heavy and other metallic elements
205 (Fig. 3). The heavy metallic element content was low, with contributions of 21.32% and 19.69%
206 to the total mass of metallic elements in $PM_{2.5}$ and PM_{10}, respectively. Fe was the most abundant
207 element. Meanwhile, the mass fractions of other metallic elements were 78.68% and 80.31%,
208 with Al, Mg, and Ca being the most abundant elements.
209
210 ***Source identification***
211 PM samples collected in the tunnel are a mixture derived from, but not limited to, vehicle exhaust,
212 tire wear, brake wear, and resuspended road dust (Lawrence, et al., 2013). The origins of OC, EC,
213 and secondary ions in the tunnel are known, based on past studies (Shen et al., 2011; Seinfeld and
214 Pandis, 2016). Therefore, this study emphasized the analysis of origins of the elements in the tunnel.
215
216 *Application of enrichment factor (EF) method*
217 Fig. 4 shows the enrichment factors of 14 elements, except for Al, P, and S (P and S were not
218 detected in the soil). The value of EF being equal to 10 is usually regarded as the criterion to

219 determine whether an element is influenced by anthropogenic sources (Voutsa and Samara, 2002).
220 EF<10 indicates that the element is not enriched, mainly originating from natural sources (soil, crust,
221 etc.), whereas EF>10 implies that the element is significantly enriched, being greatly influenced by
222 anthropogenic sources (i.e., motor vehicles in this study). It can be seen from Fig. 4 that Cu, Zn, Br,
223 and Pb were enriched (EF values were between 10 and 100), while Hg was significantly enriched
224 (EF>1000). Therefore, these elements were mainly derived from traffic-related emissions in the
225 tunnel. The EF values of Na, K, Ca, Ti, Mn, and Fe were less than 5, while the EF values of Mg, Cr,
226 and Ba were between 5 and 10. Hence, the influence of anthropogenic sources was very weak on
227 them. They mainly originated from natural sources in the tunnel, such as resuspended road dust.
228
229 *Application of principal component analysis (PCA)*
230 The mass concentration of elements from $PM_{2.5}$ and PM_{10} were used for the PCA. The dataset
231 provided KMO values of 0.652 for $PM_{2.5}$ and 0.675 for PM_{10}, ensuring their suitability for PCA. In
232 Table 5, three principal components with eigenvalues over 1were extracted, which reflected specific
233 elemental sources. All components explained 83.43% and 89.15% of the total variance in the dataset
234 of $PM_{2.5}$ and PM_{10}, respectively.

235 Component one showed the high loadings of Na, Mg, K, Ca, Ti, Cr, Mn, Fe, Cu, and Ba, with
236 medium loading of Al. Usually, Mg, Al, and Ca are regarded as typical crustal elements (Tran et al.,
237 2012). Mg and Ca can also be derived from road surface wear (Kupiainen et al., 2003).Nevertheless,
238 the EF values of all these elements were lower than 10 (Fig. 4), which suggested that they mainly
239 originated from resuspended road dust. Fe originates from crust, as well as brake wear (Sanders et al.,
240 2003). However, its EF values were lower than 10 (Fig. 4). Hence, its source was more likely to be
241 resuspended road dust. Cu and Ba are the two main additives in brake pads (Birmili et al., 2006;

242 Sanders et al., 2003). Furthermore, the EF values of Cu were greater than 10, which indicated that it
243 was significantly influenced by the traffic flow in the tunnel. Therefore, component one was strongly
244 associated with a mixed source of resuspended road dust and brake wear.

245 Component two was extracted based on the high loadings of P, S, and Zn, and medium loading of
246 Hg. In addition, a high loading of Pb was observed in $PM_{2.5}$ in component two, while medium
247 loadings were observed in PM_{10} in both component one and two. On the other hand, the correlation
248 analysis results (Table 6) showed that only five elements had good correlations with EC emissions,
249 including P, S, Zn, Hg, and Pb. Moreover, the EF values of Zn, Hg, and Pb were greater than 10 (Fig.
250 4). Hence, Pb was grouped into component two in this study. P is usually used as an additive in the
251 lubricant oil (Alves et al., 2015b). S is mainly generated by the combustion of sulfur-bearing fuel
252 (Lowenthal et al., 1994). Zn is mostly present in rubber tires. Therefore, it is regarded as a product of
253 tire wear (Degaffe and Turner, 2011). In addition, tailpipe can also emit a certain amount of Zn
254 (Huang et al., 1994). Considering that EC is mainly derived from vehicle exhaust, with all the
255 elements in component two being correlated with it, component two was attributed to a mixed source
256 of vehicle exhaust and tire wear.

257 Component three was interpreted as the exhaust emissions of diesel vehicles (DV),as it had the
258 highest loading of Br. Br has been used as a marker for PM emissions from DV (Chow, 1995). Its EF
259 values were greater than 10 (Fig. 4), which implied that it was clearly affected by the vehicles
260 traveling through the tunnel.

261

262 ***Factors influencing PM profiles***

263 Mobile source profiles of PM can be affected by a variety of factors, especially traffic conditions
264 (Nelson et al., 2008; Gillies et al., 2001; Grieshop et al., 2006). The traffic conditions in this study

265 are illustrated in Fig. 5, including uphill/downhill, vehicle volume, speed, and fuel type composition.
266 Vehicle volumes at nighttime (227 veh h^{-1}) were significantly less than those at daytime (600 veh h^{-1}),
267 as were the vehicle speeds (48.53 km h^{-1} at nighttime and 55.60 km h^{-1} at daytime). The reason was
268 the difference in the fuel type composition of vehicles during the two sampling periods. Vehicles
269 were classified into two categories according to their fuel type, including diesel vehicles (DV: buses
270 and trucks) and gasoline vehicles (GV: other vehicles such as passenger cars). There were more DV
271 in the tunnel at nighttime (69.29% of DV at nighttime and 35.94% of DV at daytime), most of them
272 being heavy-duty trucks, which moved slower than the GV under the same road conditions.
273 Moreover, vehicle speeds during the test were around 50 km h^{-1}, which indicated that the traffic was
274 free-flowing in the tunnel. Based on these traffic parameters collected in the tunnel, the running
275 direction (i.e., southbound and northbound) reflected the differences in vehicle driving conditions
276 (e.g., uphill/downhill and speed) synthetically, while the sampling period (i.e., daytime and nighttime)
277 represented the discrepancies in vehicle fleet composition (e.g., vehicle volume and fuel type).
278 Therefore, these two indexes were chosen as the influential variables. Their impacts on the contents
279 of PM species were analyzed by the Multifactorial-ANOVA. Meanwhile, according to the previous
280 PCA results (Table 5), the 17 elements were combined into three components for this analysis.
281 Furthermore, three secondary ions (NH_4^+, NO_3^-, and SO_4^{2-}) were combined into one component as
282 well.

283 It can be seen from Table 7 that the PM species of OC, EC, and elements in component one were
284 strongly influenced by the running direction in the tunnel. The fractions of OC and EC in the
285 southbound bore were both higher than those in the northbound bore (Fig. 6 and 7) due to the reverse
286 slopes in two bores. The speed was reduced, while the engine torque was increased, when vehicles

287 ascended through the southbound bore, which has a positive slope (+2.58%). Meanwhile, the fuel
288 supply was increased to guarantee the engine's power, which induced poor fuel combustion and
289 higher emissions of OC and EC. Nevertheless, the integrated contents of elements in component one
290 in the northbound bore were greater than those in the southbound bore (Fig. 8). Considering that
291 these elements mainly originated from resuspended road dust and brake wear in the tunnel, it can be
292 interpreted that more braking occurred when the vehicles descended through the northbound bore,
293 which has a negative slope (−2.58%). Moreover, the vehicle speeds were slightly higher in the
294 northbound bore during the same sampling period (Fig. 5). Therefore, more particles might be
295 produced due to a stronger disturbance of the road dust.

296 Significant influence of the sampling period was observed on the contents of the elements in
297 component three in $PM_{2.5}$, whereas its influence was not obvious in PM_{10}. The *p*-value (0.061) in
298 PM_{10} was very close to the significance level (0.05). Hence, this variable had some influence on the
299 elements in component three. Only Br was grouped in component three, with the fractions of Br
300 sampled at nighttime being higher than those collected at daytime (Fig. 9). Nevertheless, vehicle
301 volumes at nighttime were significantly less than those at daytime (Fig. 5), which presented a reverse
302 trend. Therefore, the influence of vehicle volume on the Br content was very weak. Moreover, Br is
303 primarily derived from tailpipe emissions of DV, and the proportions of DV at nighttime were
304 significantly higher than those at daytime (Fig. 5). It can be concluded that the fuel type composition
305 in the tunnel was a major factor affecting the content of Br in the PM. In addition, the running
306 direction and the sampling period did not have obvious influences on the contents of secondary ions
307 and elements in component two during this test (Table 7).

308

309 ***Comparison of PM profiles***

The mobile source profiles of PM were obtained with a mixed vehicle fleet in this study. The total mass of all the detected constituents accounted for 92.00% and 84.60% of the total mass of $PM_{2.5}$ and PM_{10}, respectively (Fig. 10). Carbonaceous species were the dominant constituent in the PM (46.06% for $PM_{2.5}$ and 37.07% for PM_{10}), while the contents of OC were higher than those of EC. The mass fractions of elements were 27.73% for $PM_{2.5}$ and 33.36% for PM_{10}. The contents of non-metallic elements were the highest in $PM_{2.5}$, while the other metallic elements were the most abundant elements in PM_{10}. Moreover, the mass contributions of secondary ions were the lowest (18.22% for $PM_{2.5}$ and 14.17% for PM_{10}).

Comparison with other PM sources

The source profiles of PM obtained in this study were compared with those from the other sources collected in northwestern China (Table 2), including ambient air ($PM_{2.5}$ profile) and road dust (PM_{10} profile; Han et al., 2014; Wang et al., 2015). The contents of OC and EC were significantly higher (2–14 times) than those from ambient air and road dust, which indicated that carbonaceous species were the primary markers of PM from vehicle emissions (Ancelet et al., 2011; Pant et al., 2017). Further, the mass fractions of three secondary ions were approximately 2 times lower than those from ambient air. A possible explanation for this difference was the weak illumination intensity in the tunnel, which partly limited the gas-to-particle conversion (Lin et al., 2010; Kang et al., 2002). The content of Fe was approximately 2 times higher than that from ambient air, which was similar to that from road dust. This implied that Fe primarily originated from the resuspended road dust in this tunnel. In addition, the fractions of P and Zn were up to 2 times higher than those from road dust, while the fractions of Cu and Pb were also slightly higher, indicating that these elements were influenced by passing vehicles, being highly enriched in the tunnel.

333
334 *Comparison with other tunnel studies*

335 The $PM_{2.5}$ profiles presented in this study were also compared with those from other tunnels in
336 China (Table 2; Cheng et al., 2010; Cui et al., 2016; Dai et al., 2015). For the same species, the mass
337 fractions presented in these tunnel tests were of the same order of magnitude. Meanwhile,
338 considerable differences were also observed, depending on the differences in vehicle type, fuel type
339 or quality, driving conditions, dust in the tunnel environment, etc. Therefore, local mobile source
340 profiles need to be established.

341 The content of OCwas higher (1.2–2.8 times) than those in the other tunnels, whereas the fraction
342 of EC was similar to the values in the other tunnels, and very close to the value in the Kuixinglou
343 tunnel. Moreover, the contents of the three secondary ions were also higher than those in the other
344 tunnels. It can be attributed to the difference in sampling depths. Most of the sampling sites in this
345 experiment were as deep as 2000 m inside the tunnel in the running direction (Fig. 1), whereas the
346 maximum sampling depths were approximately1000 m in the other tunnels. Hence, the secondary
347 conversions of OC and ions in this experiment were significantly greater.

348 For the elements in component one, the contents of Na, K, and Cr were within the range reported
349 in the other tunnel studies. The fraction of Mg was close to the value in the Wuzushan tunnel.
350 However, the elements of Ti and Cu were less than those in the other tunnels, and the elements of Al,
351 Ca, Mn, and Fe were less than those in all other tunnels, except for the Shing Mun tunnel. These
352 elements primarily originated from resuspended road dust and brake wear according to the previous
353 PCA results. A probable reason was that, the vehicle volume during this tunnel test was less (411veh
354 h^{-1} on average), with higher vehicle speed (51.84 km h^{-1} on average), whereas a volume of more
355 than 1000 veh $h^{-1}$was recorded in the other tunnels, with an average speed of 33.40 km h^{-1} in the

Zhujiang tunnel. Heavy traffic flow and lower speed would cause frequent braking, leading to a stronger disturbance of the dust on the road surface.

With regarding to the elements in component two, the contribution of Zn agreed well with the value reported in the other tunnel tests. The content of Pb was similar to the result in the Kuixinglou tunnel. Whilethe fractions of P and S were higher (4–8 times) than the results from the Shing Mun tunnel. It was potentially due to the abundant phosphorus content in the lubricant oil and higher abundance of sulfur in the vehicle fuel during this tunnel test (Alves et al., 2015b; Lowenthal et al., 1994). In addition, the element of Br in component three was consistent with the result from Shing Mun tunnel.

CONCLUSIONS

$PM_{2.5}$ and PM_{10} samples were collected in Qinling No. 1 tunnel in Xi'an, northwestern China. A comprehensive snapshot of the chemical characteristics of the traffic-related PM emissions was generated, including OC, EC, the three secondary ions of NH_4^+, NO_3^-, and SO_4^{2-}, and the 17 elements of Na, Mg, Al, P, S, K, Ca, Ti, Cr, Mn, Fe, Cu, Zn, Br, Ba, Hg, and Pb. On an average, carbonaceous species were the most dominant constituents in PM, with mass contributions of 46.06% for $PM_{2.5}$ and 37.07% for PM_{10}, while the contents of OC were higher than those of EC. The total mass fractions of secondary ions were 18.22% for $PM_{2.5}$ and 14.17% for PM_{10}, with SO_4^{2-} being the most abundant ion. Further, the sum of the mass of the 17 elements constituted 27.73% and 33.36% of the total mass of $PM_{2.5}$ and PM_{10}, respectively, with S being the most abundant element.

The sources of the different elements (e.g., exhaust and non-exhaust) in the PM were identified. The 17 elements were grouped into three components by using PCA, combined with EF. Component one comprised of the elements of Na, Mg, Al, K, Ca, Ti, Cr, Mn, Fe, Cu, and Ba, which was

attributed to the source of resuspended road dust and brake wear. Component two was related to the source of vehicle exhaust and tire wear, including the elements of P, S, Zn, Hg, and Pb. Meanwhile, component three contained only Br, which was mainly derived from the exhaust emissions of DV. Meanwhile, the emissions of OC, EC, and the elements in component one were strongly influenced by vehicle driving conditions. The fractions of OC and EC increased due to the higher engine torque and poor fuel combustion, when vehicles were ascending and at lower speeds. Meanwhile, the contents of the elements in component one increased due to frequent braking and strong disturbance of the road dust when vehicles were descending and at higher speeds. Moreover, Br was mainly affected by the vehicle fleet composition, especially the fuel type composition. The fraction of Br was higher at nighttime because of the higher proportion of DV in the fleet. However, the fractions of secondary ions and elements in component two were less influenced by these traffic parameters. In addition, the contents of OC and secondary ions might be affected by the sampling depth in the tunnel, based on the comparison between this study and other tunnel tests.

This is the first study to quantify PM profiles from mobile sources by using tunnel methodology in Xi'an, northwestern China. The results can complement the studies conducted in various parts of China, to acquire a better comprehension of PM pollution due to the road traffic in this country.

ACKNOWLEDGEMENTS

This work was supported by the National Natural Science Foundation of China (No. 21607014, No. 51478045), the Foundation of Science and Technology Coordinating Innovative Engineering Projects of Shaanxi Province (No. 2016KTZDSF-02-01), and the Natural Science Basic Research Plan in Shaanxi Province of China (No. 2017JM7007).

SUPPLEMENTARY MATERIAL

Supplementary data associated with this article can be found in the online version at XXXX

REFERENCES

Alves, C.A., Gomes, J., Nunes, T., Duarte, M., Calvo, A., Custódio, D., Pio, C., Karanasiou, A., 安 and Querol, X. (2015a). Size-segregated particulate matter and gaseous emissions from motor vehicles in a road tunnel. *Atmos. Res.* 153: 134–144.

Alves, C. A., Barbosa, C., Rocha, S., Calvo, A., Nunes, T., Cerqueira, M., Pio, C., Karanasiou, A. Querol, X. (2015b). Elements and polycyclic aromatic hydrocarbons in exhaust particles emitted by light-duty vehicles. *Environ. Sci. Pollut. Res. Int.* 22 (15): 1-17.

Alves, C.A., Oliveira, C., Martins, N., Mirante, F., Caseiro, A., Pio, C., Matos, M., Silva, H.F., Oliveira, C., and Camoes, F. (2016). Road tunnel, roadside, and urban background measurements of aliphatic compounds in size-segregated particulate matter. *Atmos. Res.* 168: 139–148.

Ancelet, T., Davy, P.K., Trompetter, W.J., Markwitz, A., and Weatherburn, D.C. (2011). Carbonaceous aerosols in an urban tunnel. *Atmos. Environ.* 45: 4463–4469.

Birmili, W., Allen, A.G., Bary, F., and Harrison, R.M. (2006). Trace metal concentrations and water solubility in size-fractionated atmospheric particles and influence of road traffic. *Environ. Sci. Technol.* 40(4): 1144–1153.

Cevik, F., Goksu, M.Z.L., Derici, O.B., and Findik, O. (2009). An assessment of metal pollution in surface sediments of Seyhan dam by using enrichment factor, geoaccumulation index and statistical analyses. *Environ. Monit. & Assess.* 152(1-4): 309-317.

Cheng, Y., Lee, S.C., Ho, K.F., Chow, J.C., Watson, J.G., Louie, P.K.K., Cao, J.J., and Hai, X. (2010). Chemically speciated on-road $PM_{2.5}$ motor vehicle emission factors in Hong Kong. *Sci.*

Total Environ. 408 (7): 1621–1627.

Chiang, H.L., and Huang, Y.S. (2009). Particulate matter emissions from on-road vehicles in a freeway tunnel study. *Atmos. Environ.* 43 (26): 4014–4022.

Chow, J.C., 1995. Measurement methods to determine compliance with ambient air quality standards for suspended particles. *J. Air & Waste Manage. Assoc.* 45: 320–382.

Cui, M., Chen, Y.J., Tian, C.G., Zhang, F., Yan, C.Q., and Zheng, M. (2016). Chemical composition of $PM_{2.5}$ from two tunnels with different vehicular fleet characteristics. *Sci. Total Environ.* 550: 123-132.

Dai, S., Bi, X., Chan, L. Y., He, J., Wang, B., Wang, X., Peng, P., Sheng, G., and Fu, J. (2015). Chemical and stable carbon isotopic composition of $PM_{2.5}$ from on-road vehicle emissions in the PRD region and implications for vehicle emission control policy. *Atmos. Chem. Phys.* 15(6): 3097–3108.

Degaffe, F.S., and Turner, A. (2011). Leaching of zinc from tire wear particles under simulated estuarine conditions. *Chemosphere.* 85(5): 738–743.

Delfino, R.J., Staimer, N., Tjoa, T., Polidori, A., Arhami, M., Gillen, D.L., Kleinman, M.T., Vaziri, N.D., Longhurst, J., Zaldivar, F., and Sioutas, C. (2008). Circulating biomarkers of inflammation, antioxidant activity, and platelet activation are associated with primary combustion aerosols in subjects with coronary artery disease. *Environ. Health Perspect.* 116: 898–906.

Deng, X.J., Wu, D., Yu, J.Z., Lau A.K.H., and Li F. (2013). Characterization of secondary aerosol and its extinction effects on visibility over the Pearl River Delta Region, China. *J. Air & Waste Manage. Assoc.* 63: 1012–1021.

Franco, V., Kousoulidou, M., Muntean, M., Ntziachristos, L., Hausberger, S., and Dilara, P. (2013).

446 Road vehicle emission factors development: a review. *Atmos. Environ.* 70: 84–97.

447 Handler, M., Puls, C., Zbiral, J., Marr, I., Puxbaum, H., and Limbeck, A. (2008). Size and
448 composition of particulate emissions from motor vehicles in the Kaisermuhlen-Tunnel, Vienna.
449 *Atmos. Environ.* 42 (9): 2173–2186.

450 Gillies, J.A., Gertler, A.W., Sagebiel, J.C., and Dippel, W.A. (2001). On-road particulate matter
451 ($PM_{2.5}$ and PM_{10}) emissions in the Sepulveda Tunnel, Los Angeles, California. *Environ. Sci.*
452 *Technol.* 35(6): 1054–63.

453 Grieshop, A.P., Lipsky, E.M., Pekney, N.J., Takahama, S., and Robinson, A.L. (2006). Fine particle
454 emission factors from vehicles in a highway tunnel: effects of fleet composition and season. *Atmos.*
455 *Environ.* 40: S287–298.

456 Haase, R.F., and Ellis, M.V. (1987). Multivariate analysis of variance. *Journal of Counseling*
457 *Psychology.* 34 (4): 404-413.

458 Han, J.B., Han, B., Li, P.H., Kong, S.F., Bai, Z.P., Han, D.H., Dou, X.Y., and Zhao, X.D. (2014).
459 Chemical characterizations of PM_{10} profiles for major emission sources in Xining, northwestern
460 China. *Aerosol Air Qual. Res.* 14: 1017–1027.

461 He, L.Y., Hu, M., Zhang, Y.H., Huang, X.F., and Yao, T.T. (2008). Fine particle emissions from
462 on-road vehicles in the Zhujiang Tunnel, China. *Environ. Sci. Technol.* 42: 4461–4466.

463 Ho, K.F., Ho, S.S.H., Lee, S.C., Cheng, Y., Chow, J.C., Watson, J.G., Louie, P.K.K., and Tian, L.W.
464 (2009). Emissions of gas- and particle-phase polycyclic aromatic hydrocarbons (PAHs) in the
465 Shing Mun Tunnel, Hong Kong. *Atmos. Environ.* 43 (40): 6343–6351.

466 Huang, X., Olmez, L., Aras, N.K., and Gordon, G.E. (1994). Emissions of trace elements from motor
467 vehicles: potential marker elements and source composition profile. *Atmos. Environ.* 28(8):

1385–1391.

Huang, X.F., Yu, J.Z., He, L.Y., and Hu, M. (2006). Size distribution characteristics of elemental carbon emitted from Chinese vehicles: Results of a tunnel study and atmospheric implications. *Environ. Sci. Technol.* 40: 5355–5360.

Kang, C.，Han, J., and Sunwoo, Y. (2002)．Hydrogen peroxide concentrations in the ambient air of Seoul，Korea．*Atmos. Environ.* 36(35): 5509–5516．

Kupiainen, K.J., Tervahattu, H., and Räisänen, M. (2003). Experimental studies about the impact of traction sand on urban road dust composition. *Sci. Total Environ.* 308: 175–184.

Lawrence, S., Sokhi, R., Ravindra, K., Mao, H.J., Prain, H.D., and Bull, I.D. (2013). Source apportionment of traffic emissions of particulate matter using tunnel measurements. *Atmos. Environ.* 77: 548–557.

Larsen, R.K., and Baker, J.E. (2003). Source apportionment of polycyclic aromatic hydrocarbons in the urban atmosphere: a comparison of three methods. *Environ. Sci. Technol.* 37: 1873-1881.

Lin, Y.C.，Cheng, M.T., Lin, W.H., Lan, Y.Y., and Tsuang, B.J. (2010). Causes of the elevated nitrate aerosol levels during episodic days in Taichung urban area, TaiWan．*Atmos. Environ.* 44(13): 1632–1640．

Liu, W.T., Ma, C.M., Liu, I.J., Han, B.C., Chuang, H.C., and Chuang, K.J. (2015a). Effects of commuting mode on air pollution exposure and cardiovascular health among young adults in Taipei, Taiwan. Int. J. Hyg. *Environ. Health.* 218 (3): 319–323.

Liu, Y., Gao, Y., Yu, N., Zhang, C.K., Wang, S.Y., Ma, L.M., Zhao, J.F., and Lohmann, R. (2015b). Particulate matter, gaseous and particulate polycyclic aromatic hydrocarbons (PAHs) in an urban traffic tunnel of China: Emission from on-road vehicles and gas-particle partitioning.

Chemosphere. 134: 52–59.

Liu, Y., Wang, S.Y., Lohmann, R., Yu, N., Zhang, C.K., Gao, Y., Zhao, J.F., and Ma, L.M. (2015c). Source apportionment of gaseous and particulate PAHs from traffic emission using tunnel measurements in Shanghai, China. *Atmos. Environ.* 107: 129–136.

Lowenthal, D.H., Zielinska, B., Chow, J.C., Watson, J.G., Gautam, M., Ferguson, D.H., Neuroth, G.R., and Stevens, K.D. (1994). Characterization of heavy-duty diesel vehicle emissions. *Atmos. Environ.* 28(4): 731–743.

Ministry of Environmental Protection of the People's Republic of China (MEPC). China vehicle environmental management annual report. http://www.zhb.gov.cn/gkml/hbb/qt/201706/t20170603_415265.htm, Last Access: 2 February 2018.

Na, K., Biswas, S., Robertson, W., Sahay, K., Okamoto, R., Mitchell, A., and Lemieux, S. (2015). Impact of biodiesel and renewable diesel on emissions of regulated pollutants and greenhouse gases on a 2000 heavy duty diesel truck. *Atmos. Environ.* 107: 307–314.

National Environmental Monitoring Center of China (NEMCC), 1990. *Chinese soil element background content.* Chinese Environment Science Press, Beijing.

Nelson, P.F., Tibbett, A.R., and Day, S.J. (2008). Effects of vehicle type and fuel quality on real world toxic emissions from diesel vehicles. *Atmos. Environ.* 42(21): 5291–303.

NIOSH. (2003). Manual of analytical methods (NMAM). In: O'Connor, P.F., Schlecht, P.C. (Eds.), Monitoring of Diesel Particulate Exhaust in the Workplace, Chapter Q, Third Supplement to NMAM, fourth ed. NIOSH, Cincinnati, OH. DHHS (NIOSH) Publication No. 2003-154.

Pant, P., Shi, Z.B., Pope, F.D., and Harrison, R.M. (2017). Characterization of traffic-related

512 particulate matter emissions in a road tunnel in Birmingham, UK: trace metals and organic
513 molecular markers. *Aerosol Air Qual. Res.* 17: 117–130.
514 Pietikainen, M., Valiheikki, A., Oravisjarvi, K., Kolli, T., Huuhtanen, M., Niemi, S., Virtanen, S.,
515 Karhu, T., and Keiski, R.L. (2015). Particle and NO_x emissions of a non-road diesel engine with
516 an SCR unit: the effect of fuel. Renew. *Energy.* 77: 377–385.
517 Pio, C., Mirante, F., Oliveira, C., Matos, M., Caseiro, A., Oliveira, C., Querol, X., Alves, C., Martins,
518 N., and Cerqueira, M. (2013). Size-segregated chemical composition of aerosol emissions in an
519 urban road tunnel in portugal. *Atmos. Environ.* 71: 15–25.
520 Sakan, S.M., Dević, G.J., Relić, D.J., Andelković, I.B., Sakan, N.M., and Dordevic, D.S. (2014).
521 Environmental assessment of heavy metal pollution in freshwater sediment, Serbia. *Clean-Soil,*
522 *Air, Water*. 43(6): 838–845.
523 Sanders, P.G., Xu, N., Dalka, T.M., and Maricq, M.M. (2003). Airborne brake wear debris: size
524 distribution, composition, and a comparison of dynamometer and vehicle tests. *Environ. Sci.*
525 *Technol.* 37(18): 4060–4069.
526 Seinfeld, J.H., and Pandis, S.N. (2016). *Atmospheric chemistry and physics: from air pollution to*
527 *climate change*. John Wiley & Sons, Inc., Hoboken.
528 Shen, Z.X., Cao, J.J., Liu, S.X., Zhu, C.S., Wang, X., Zhang, T., Xu, H.M., and Hu, T.F. (2011).
529 Chemical composition of PM_{10} and $PM_{2.5}$ collected at ground level and 100 meters during a strong
530 winter-time pollution episode in Xi'an, China. *J. Air & Waste Manage. Assoc.* 61: 1150–1159.
531 Spira-Cohen, A., Chen, L.C., Kendall, M., Lall, R., and Thurston, G.D. (2011). Personal exposures to
532 traffic-related air pollution and acute respiratory health among Bronx schoolchildren with asthma.
533 Environ. *Health Perspect.* 119: 559–565.

534 Thorpe, A., and Harrison, R. M. (2008). Sources and properties of non-exhaust particulate matter
535 from road traffic: A review. *Sci. Total Environ.* 400: 270–282.
536 Tran, D.T., Alleman, L.Y., Coddeville, P., and Galloo, J.C. (2012). Elemental characterization and
537 source identification of size resolved atmospheric particles in French classrooms. *Atmos. Environ.*
538 54(5): 250–259.
539 Voutsa, D., and Samara, C. (2002). Labile and bioaccessible fractions of heavy metals in the airborne
540 particulate matter from urban and industrial areas. *Atmos. Environ.* 36(22): 3583–3590.
541 Wang, P., Cao, J.J., Shen, Z.X., Han, Y.M., Lee, S.C., Huang, Y., Zhu, C.S., Wang, Q.Y., Xu, H.M.,
542 and Huang, R.J. (2015). Spatial and seasonal variations of $PM_{2.5}$ mass and species during 2010 in
543 Xi'an, China. *Sci. Total Environ.* 508: 477–487.
544 Wolny, S., and Kedzia, J. (2008). Application of multifactorial variance analysis for assessment of
545 temperature influence on selected parameters of recovery voltage of paper-oil insulation. *Przeglad*
546 *Elektrotechniczny.* 84(10): 218-221.
547 Yao, Z.L., Shen, X.B., Ye, Y., Cao, X.Y., Jiang, X., Zhang, Y.Z., and He, K.B. (2015). On-road
548 emission characteristics of VOCs from diesel trucks in Beijing, China. *Atmos. Environ.* 103:
549 87–93.
550 Yu, S., Dennis, R.L., Bhave, P.V., and Eder, B.K. (2004). Primary and secondary organic aerosols
551 over the United States: estimates on the basis of observed organic carbon (OC) and elemental
552 carbon (EC), and air quality modeled primary OC/EC ratios. *Atmos. Environ.* 38 (31): 5257–5268.
553 Zhang, F., Chen, Y.J., Tian, C.G., Wang, X.P., Huang, G.P., Fang, Y., and Zong, Z. (2014).
554 Identification and quantification of shipping emissions in Bohai Rim, China. *Sci. Total Environ.* S
555 497–498: 570–577.

Zhang, Y. Z., Yao, Z. L., Shen, X. B., Liu H., and He K. B. (2015a). Chemical characterization of $PM_{2.5}$ emitted from on-road heavy-duty diesel trucks in China. *Atmos. Environ.* 122: 885–891.

Zhang, Y.L., Wang, X.M., Li, G.H., Yang, W.Q., and Huang, Z.H. (2015b). Emission factors of fine particles, carbonaceous aerosols and traces gases from road vehicles: Recent tests in an urban tunnel in the Pearl River Delta, China. *Atmos. Environ.* 122: 876–884.

Zhao, Q., Yu, Q., and Chen, L.M. (2010). Particulate matter and particle-bound polycyclic aromatic hydrocarbons in the Dapu road tunnel in Shanghai. *Int. J. Environ. Pollut.* 41: 21–37.

572 **List of table titles**

573 **Table 1.** Summary of the samples in the tunnel

574 **Table 2.** Chemical compositions of PM in several studies (%)

575 **Table 3.** Analysis of the influence of particle size on PM composition

576 **Table 4.** Mass fraction distribution of elements

577 **Table 5.** Factor loadings of elements in the PCA (only loadings >0.5 are shown)

578 **Table 6.** Correlation coefficients between elements and EC

579 **Table 7.** Influence analysis of traffic conditions on PM profiles

580

581 **Table 1.** Summary of the samples in the tunnel

Site	Bore	Sampling number	Sampling period
#1	Southbound	6	Daytime or Nighttime
#2		2	
#3		2	
#4		2	
#1	Northbound	4	
#2		2	
#3		2	

582

583

584 **Table 2.** Chemical compositions of PM in several studies (%)

City	Xi'an		Xi'an	Xining	Hong Kong	Guangzhou	Yantai	
Year	2016		2010	2010	2003	2013	2014	
Source	Qinling No.1 tunnel		Ambient air	Road dust	Shing Mun tunnel	Zhujiang tunnel	Wuzushan tunnel	Kuixinglou tunnel
References	This study		Wang et al. (2015)	Han et al. (2014)	Cheng et al. (2010)	Dai et al. (2015)	Cui et al. (2016)	
PM	$PM_{2.5}$	PM_{10}	$PM_{2.5}$ [a]	PM_{10}	$PM_{2.5}$ [b]	$PM_{2.5}$ [b]	$PM_{2.5}$ [b]	$PM_{2.5}$ [b]
OC	34.10±6.43	28.48±16.02	13.04	5.98±1.86	27.25	18.07	27.67	17.70
EC	11.96±4.30	8.59±3.81	4.70	0.60±0.13	50.23	17.75	32.10	10.36
NH_4^+	3.19±2.04	2.14±1.54	5.82		2.14	0.18	0.87	0.14
NO_3^-	6.05±4.42	4.30±2.97	12.48	0.06±0.06	0.84	0.11	3.28	3.65
SO_4^{2-}	8.98±4.82	7.73±4.40	16.20	1.38±0.83	5.42	0.66	3.71	3.02
Na	1.48±1.20	3.19±2.67		0.84±0.24	0.76	3.82	0.37	0.32
Mg	2.29±1.27	4.17±3.91		1.71±0.39	0.27	0.54	2.01	1.13
Al	2.77±1.57	3.67±1.83		5.16±0.62	0.17	3.41		
P	0.24±0.14	0.26±0.11		0.11±0.03	0.05			
S	16.00±7.64	12.89±4.77			2.06			
K	0.48±0.27	0.59±0.24		1.55±0.17	0.22	0.37	0.97	0.59
Ca	1.85±1.27	4.27±2.40		9.84±2.33	0.42	2.09	5.42	2.12
Ti	0.04±0.03	0.08±0.04	0.07	0.26±0.05	0.06		0.21	0.09
Cr	0.01±0.01	0.02±0.02		0.02±0.01	0.01	0.01	0.01	0.14
Mn	0.03±0.03	0.06±0.04	0.07	0.08±0.01	0.02	0.09	0.09	0.09
Fe	2.14±1.86	3.56±2.87	0.98	2.74±0.49	0.73	4.23	4.59	4.19
Cu	0.02±0.02	0.04±0.03		0.03±0.04	0.04	0.10	0.04	0.11
Zn	0.19±0.04	0.26±0.05	0.98	0.10±0.08	0.15	0.17	0.17	0.11
Br	0.004±0.004	0.003±0.002			0.004			
Ba	0.14±0.13	0.27±0.23			0.06			
Hg	0.008±0.005	0.011±0.009						
Pb	0.03±0.02	0.04±0.02	0.21	0.03±0.01	0.02	0.01	0.01	0.03

585 [a] Mass fractions of each species were calculated based on the mass concentrations of $PM_{2.5}$ and its corresponding species.

586 [b] Mass fractions of each species were calculated based on the emission factors of $PM_{2.5}$ and its corresponding species.

587

588 **Table 3.** Analysis of the influence of particle size on PM composition

Species	*F*-value	*p*-value	Species	*F*-value	*p*-value
OC	1.198	0.281	Ca	16.942	**0.000**
EC	6.904	**0.012**	Ti	16.160	**0.000**
NH_4^+	2.872	0.098	Cr	3.157	0.084
NO_3^-	0.036	0.851	Mn	3.896	0.056
SO_4^{2-}	1.535	0.223	Fe	3.919	0.055
Na	10.012	**0.003**	Cu	5.481	**0.025**
Mg	5.724	**0.022**	Zn	18.967	**0.000**
Al	2.925	0.095	Br	0.271	0.606
P	0.019	0.890	Ba	4.420	**0.042**
S	2.393	0.130	Hg	2.189	0.147
K	2.598	0.115	Pb	1.381	0.247

589

590

591 **Table 4.** Mass fraction distribution of elements (%)

Mass fraction	>5%	1–5%	0.1–1%	0.01–0.1%	<0.01%
$PM_{2.5}$	S	Al, Mg, Fe, Ca, Na	K, P, Zn, Ba	Ti, Pb, Mn, Cu, Cr	Hg, Br
PM_{10}	S	Ca, Mg, Al, Fe, Na	K, Ba, P, Zn	Ti, Mn, Pb, Cu, Cr	Hg, Br

592

593

594

595 **Table 5.** Factor loadings of elements in the PCA (only loadings >0.5 are shown)

Element	$PM_{2.5}$			PM_{10}		
	Component 1	Component 2	Component 3	Component 1	Component 2	Component 3
Na	0.844			0.897		
Mg	0.772			0.941		
Al	0.516			0.599		
P		0.889			0.926	
S		0.919			0.970	
K	0.770			0.926		
Ca	0.908			0.944		
Ti	0.922			0.947		
Cr	0.971			0.986		
Mn	0.950			0.948		
Fe	0.982			0.985		
Cu	0.737			0.753		
Zn		0.910			0.841	
Br			0.884			0.951
Ba	0.917			0.978		
Hg		0.646			0.700	
Pb		0.836		0.660	0.533	
Variance (%)	46.77	26.62	10.04	56.61	24.20	8.34

596

597

598 **Table 6.** Correlation coefficients between elements and EC

Element	EC		Element	EC	
	$PM_{2.5}$	PM_{10}		$PM_{2.5}$	PM_{10}
Na	−0.123	0.237	Mn	−0.129	−0.016
Mg	−0.150	0.022	Fe	−0.024	0.106
Al	0.237	0.425	Cu	0.378	0.473
P	**0.733**	**0.902**	Zn	**0.723**	**0.866**
S	**0.555**	**0.897**	Br	0.227	0.271
K	−0.210	0.310	Ba	0.198	0.069
Ca	0.151	0.310	Hg	**0.555**	**0.506**
Ti	0.155	0.274	Pb	**0.562**	**0.637**
Cr	−0.059	0.062			

599

600

601

602 **Table 7.** Influence analysis of traffic conditions on PM profiles

PM	Influential variables	OC		EC		Secondary ions	
		F-value	*p*-value	*F*-value	*p*-value	*F*-value	*p*-value
$PM_{2.5}$	Running direction	3.695	**0.045**	33.079	**0.000**	0.492	0.495
	Sampling period	0.001	0.973	0.036	0.853	0.009	0.927
	Running direction × Sampling period	0.012	0.913	0.673	0.426	0.493	0.494
PM_{10}	Running direction	5.005	**0.042**	14.726	**0.002**	0.933	0.350
	Sampling period	0.156	0.699	1.001	0.334	0.011	0.919
	Running direction × Sampling period	0.290	0.599	1.971	0.182	0.542	0.474
PM	Influential variables	Elements					
		Component 1		Component 2		Component 3	
		F-value	*p*-value	*F*-value	*p*-value	*F*-value	*p*-value
$PM_{2.5}$	Running direction	73.103	**0.000**	1.063	0.320	0.180	0.678
	Sampling period	0.854	0.371	0.200	0.662	4.658	**0.049**
	Running direction × Sampling period	1.102	0.312	0.063	0.805	3.621	0.078
PM_{10}	Running direction	37.034	**0.000**	0.429	0.523	0.225	0.642
	Sampling period	1.725	0.210	0.182	0.676	4.143	0.061
	Running direction × Sampling period	0.014	0.908	0.074	0.790	0.764	0.397

603

List of figure captions

Fig.1. Location of Qinling No.1 tunnel and its sketch map

Fig. 2. Mass fractions of metallic and non-metallic elements

Fig. 3. Mass fractions of heavy metallic and other metallic elements

Fig. 4. Enrichment factors of elements in PM

Fig. 5. Traffic conditions during the tunnel test

Fig. 6. Mass fractions of OC in the two directions

Fig. 7. Mass fractions of EC in the two directions

Fig. 8. Mass fractions of elements in component one in the two directions

Fig. 9. Mass fractions of Br during the two sampling periods

Fig. 10. Mass fractions of PM species in the tunnel

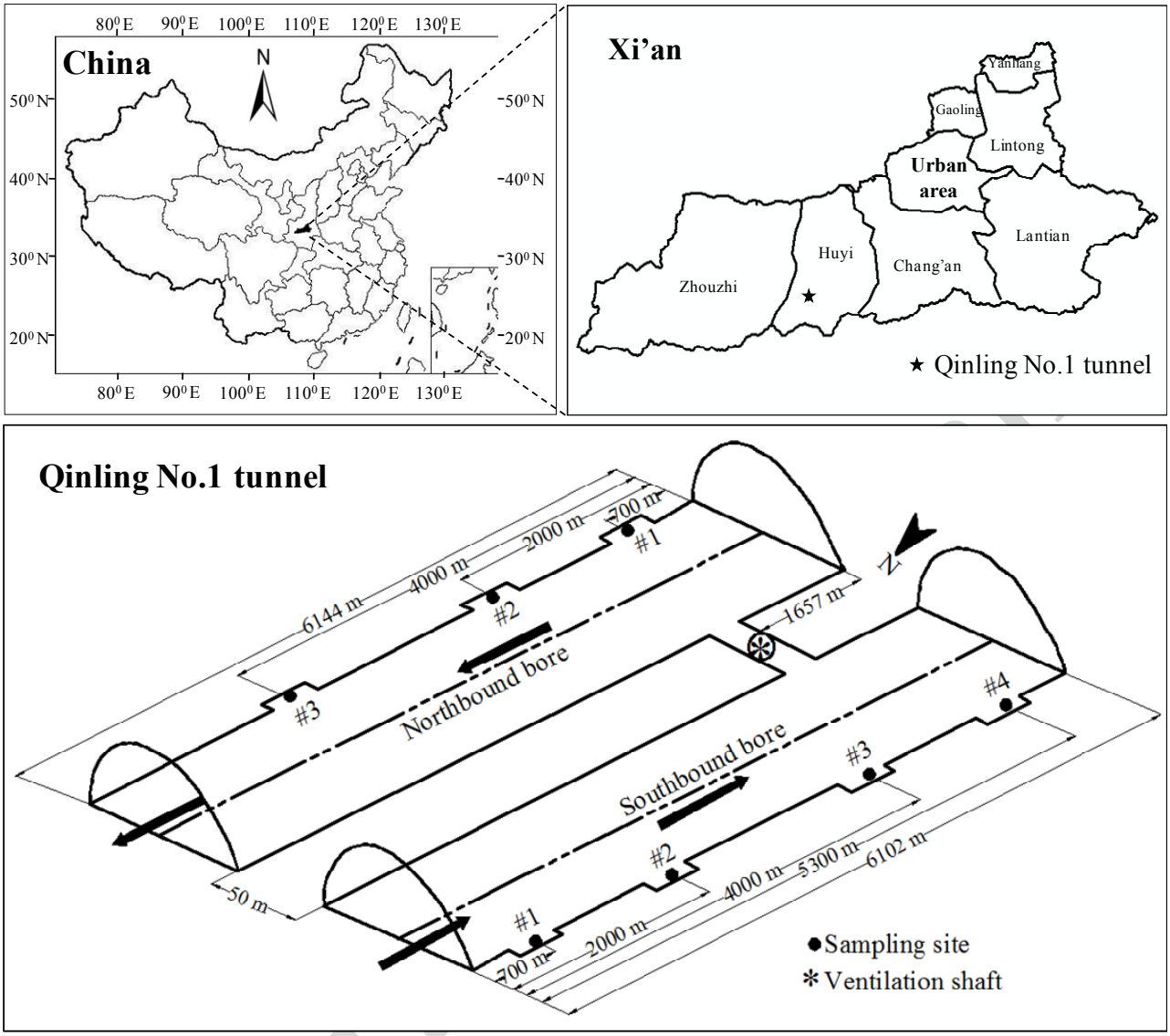

Fig.1. Location of Qinling No.1 tunnel and its sketch map

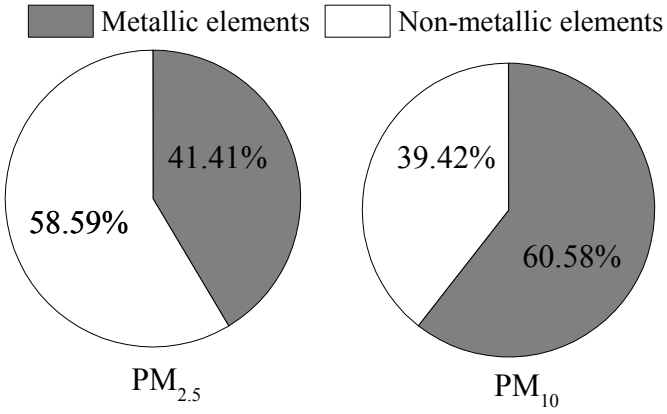

623

624 **Fig. 2.** Mass fractions of metallic and non-metallic elements (Metallic elements: Na, Mg, Al, K, Ca,
625 Ti, Cr, Mn, Fe, Cu, Zn, Ba, Hg, and Pb; Non-metallic elements: P, S, and Br)

626

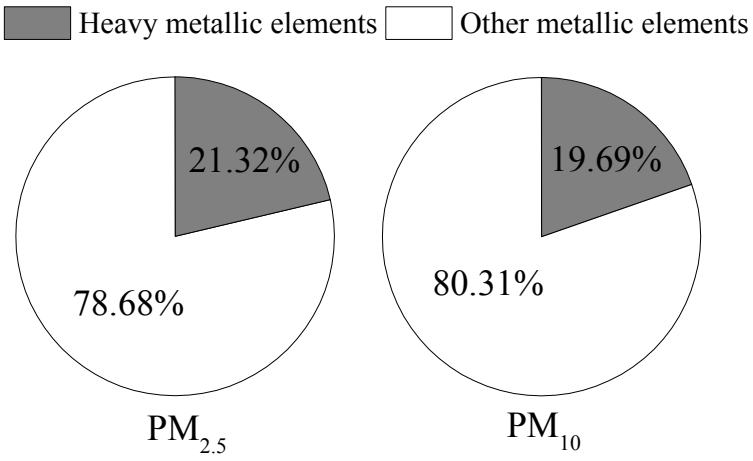

627

628 **Fig. 3.** Mass fractions of heavy metallic and other metallic elements (Heavy metallic elements: Cr,
629 Mn, Fe, Cu, Zn, Hg, and Pb; Other metallic elements: Na, Mg, Al, K, Ca, Ti, and Ba)

630

631

632

633

634

635

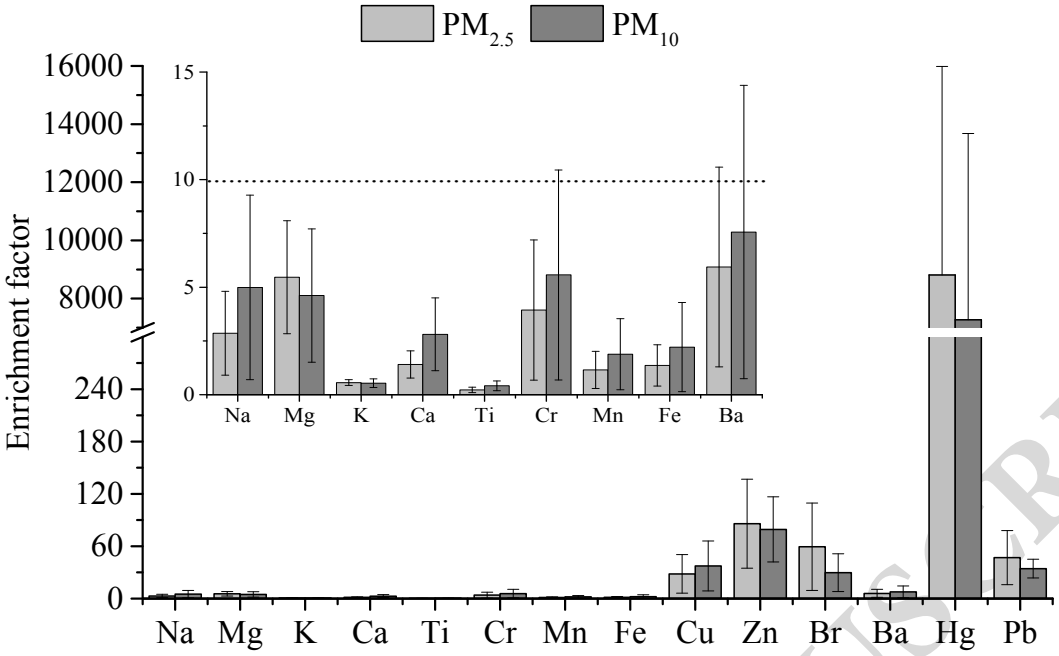

Fig. 4. Enrichment factors of elements in PM

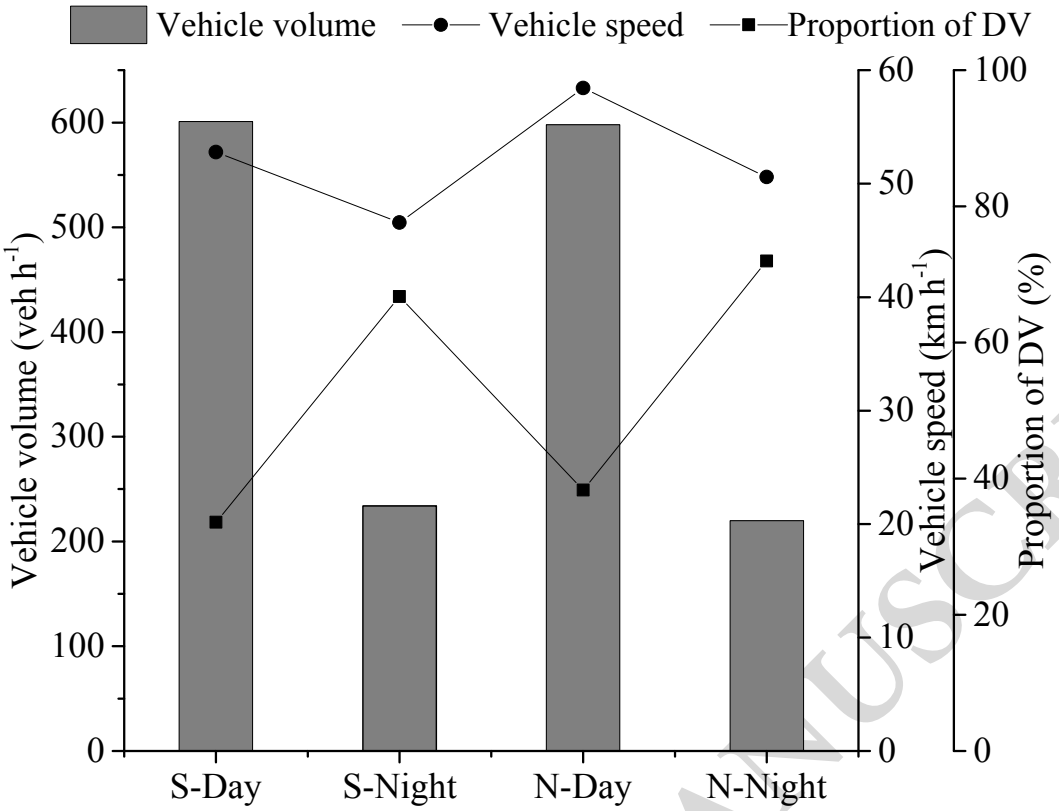

Fig. 5. Traffic conditions during the tunnel test (S: southbound, N: northbound, Day: daytime, Night: nighttime)

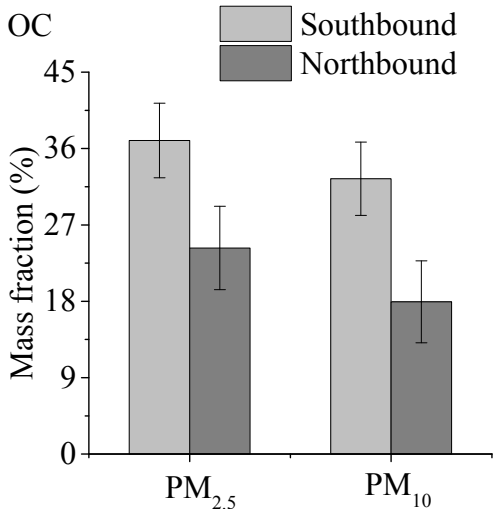

Fig. 6. Mass fractions of OC in the southbound and northbound bore

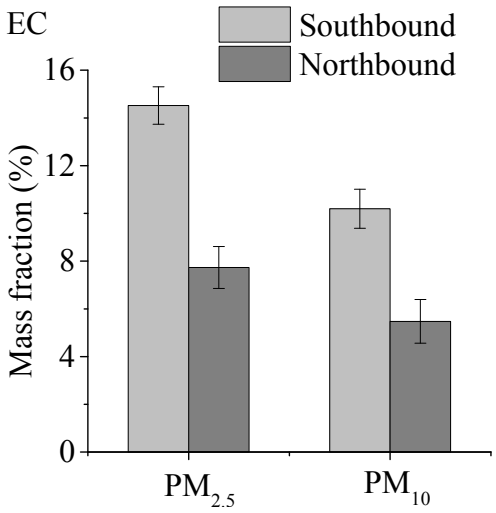

Fig. 7. Mass fractions of EC in the southbound and northbound bore

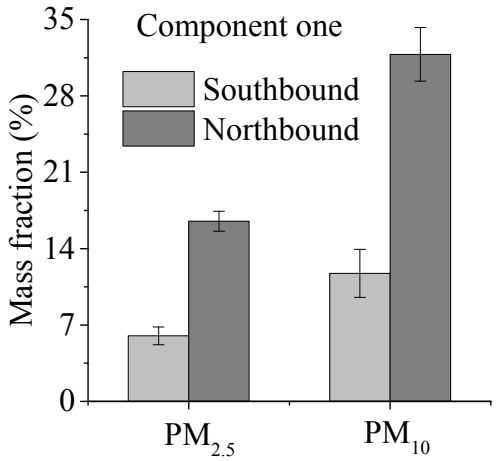

Fig. 8. Mass fractions of elements in component one in the southbound and northbound bore (Component one include elements of Na, Mg, Al, K, Ca, Ti, Cr, Mn, Fe, Cu, and Ba)

665

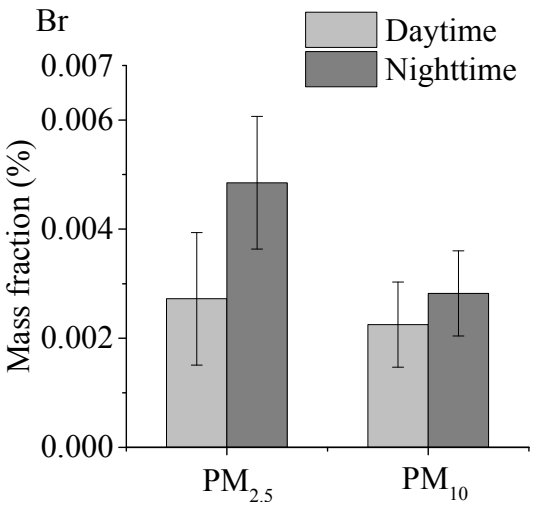

666

667 **Fig. 9.** Mass fractions of Br at daytime and nighttime

668

669

670

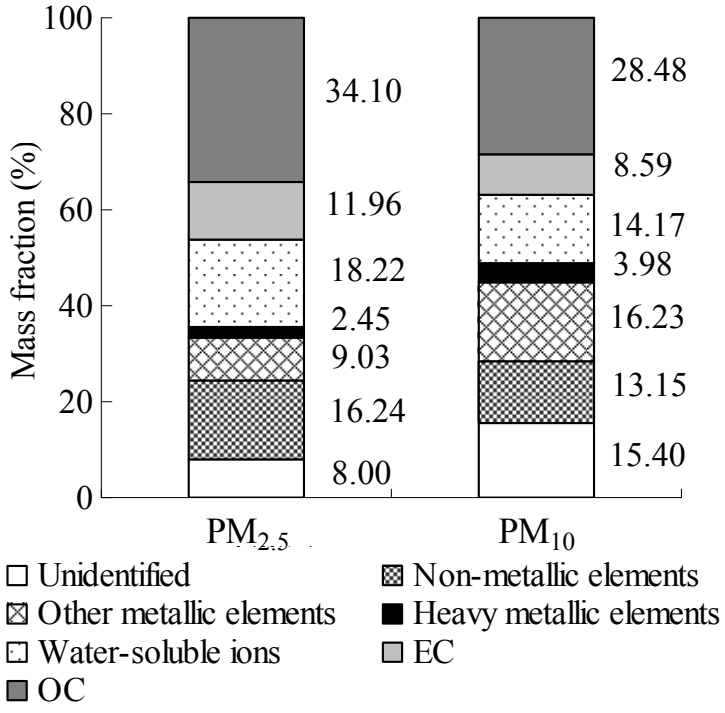

671

672 **Fig. 10.** Mass fractions of PM species in the tunnel